An Electrochemical Sensor for Simultaneous Stripping Determination of Cd(II) and Pb(II) Based on Gold Nanoparticles Functionalized β-cyclodextrin-graphene Hybrids

Xiaoli Qin[1], Daili Tang[1], Yunxiang Zhang[1], Yongbing Cheng[1], Fang He[2], Zhaohong Su[1,*] and Hongmei Jiang[1,*]

[1] College of Chemistry and Material Science, Hunan Agricultural University, Changsha 410128, China
[2] College of Pharmacy, Shaoyang University, Shaoyang 422000, China
[*]E-mail: zhaohongsu@hunau.edu.cn ; jhmndcn@hunau.edu.cn

A simple and sensitive electrochemical sensor was reported for the simultaneous detection of Cd(II) and Pb(II) using gold nanoparticles functionalized β-cyclodextrin (β-CD)-graphene hybrids (AuNPs-CD-GS) as the sensing platform. The disperse AuNPs-CD-GS are fabricated by a simple one-pot synthesis using hydrazine and β-CD as reducing agents to reduce the graphene oxide and gold ions. A homogeneous AuNPs on the CD-GS was obtained and the concentration of $HAuCl_4$ was considered. This nanocomposite not only presents the excellent electrical properties of AuNPs and GS but also shows high capture capability due to the strong adsorption uptake of Cd^{2+} and Pb^{2+} on β-CD. Under the optimal conditions, the stripping peak currents are linearly related to the concentrations of Cd^{2+} and Pb^{2+} over the range from 40 - 1200 μg L^{-1}. The simultaneous and sensitive detection of Cd^{2+} and Pb^{2+} in real water samples was also conducted and the satisfactory results were obtained.

1. INTRODUCTION

Nowadays, heavy metal ions such as Cd^{2+}, Pb^{2+} in environment are not biodegradable and can accumulate in the human body leading to damage of the central nervous, immune and reproductive systems [1-3]. Therefore, it is urgently necessary to develop simple, rapid and sensitive analytical methods for precise quantification of them in the environment. To date, various analytical techniques including optical methods [4, 5], atomic absorption spectrometry [6], mass spectrometry [7] and electrochemical methods [8, 9] have been already introduced for the simultaneous analysis of heavy metal ions. However, electrochemical methods are considered as an effective method for simultaneous determination of Cd^{2+} and Pb^{2+} due to the excellent sensitivity, low-cost instrumentation and ease of

portability [10, 11]. Accordingly, many novel materials, e.g. β-cyclodextrin (β-CD), gold nanoparticles (AuNPs), graphene and carbon nanotubes, have been used to construction of heavy metals sensor to output and amplify the analytical signals due to their unique optical, electrochemical, structural property, and/or high adsorption capability [12, 13].

β-CD, a unique oligosaccharide composed of seven glucose units, is toroidal in shape with a hydrophilic exterior and a hydrophobic inner cavity and has been widely used to develop various sensors [14-16]. It is a water-solution and environmentally friendly material which can improve the stability and solubility of functional materials. For instance, Xia et al reported an eco-friendly method to fabricate monodisperse β-CD modified gold nanoparticle (AuNP) by the proposed one-step colloidal synthesis method using β-CD as both reducing agents and stabilizers [14]. Furthermore, the β-CD functional materials can be utilized in electrochemical sensors for heavy metal detection [17] and adsorbents of the heavy metal ions due to forming inclusive complexes with the heavy metal ions [18, 19].

Graphene sheet (GS), as a new 2D enhanced carbon material, can be produced by the chemically reduced graphene oxide (GO) and has been applied for developing high-performance electrochemical devices owing to its extraordinary electronic transport property, electrocatalytic activity and high surface area [20-24]. β-CD-functionalized GS (CD-GS) with enrichment capability and high supramolecular recognition has been intensively explored for the applications in the fields of eletrocatalysis and sensors [16, 25]. Moreover, more enhanced electrochemical performances for electrochemical sensing platform have been attained by incorporation of the CD-GS with AuNPs, because the AuNPs could provide the large surface area, excellent electrical conductivity and good biocompatibility [15, 26, 27]. Guo et al demonstrated a new electrochemical thrombin aptasensor based on thio-β-CD functionalized graphene-AuNP hybrids with strong supramolecular capability [27]. However, to the best of our knowledge, there are no published data for application of AuNPs-CD-GS as platform in the fabrication of electrochemical sensor for Cd^{2+} and Pb^{2+} simultaneous analysis.

In the present work, we report a simple and highly sensitive electrochemical sensor for Cd^{2+} and Pb^{2+} simultaneous analysis, on the basis of a facile one-pot method for controlled synthesis of AuNPs functionalized CD-GS composites. During the synthesis process, a homogeneous AuNPs on the CD-GS was obtained and the concentration of $HAuCl_4$ was explored in detail. Specifically, β-CD not only acts as the stabilizer, dispersant and reducing agents to reduce the gold ions but also can accumulate and bind more Cd^{2+} and Pb^{2+} on the electrode surface by the hydroxyl groups on its hydrophilic edge. Major steps for preparing AuNPs-CD-GS and sensing Cd^{2+} and Pb^{2+} by electrochemical strategy are depicted in Scheme 1. Transmission electron microscopy (TEM), scanning electron microscopy (SEM), Fourier transform infrared spectroscopy (FT-IR) and X-ray photoelectron spectroscopy (XPS) were used to investigate the morphology and properties of this nanocomposites. Under the optimal conditions, this proposed AuNPs-CD-GS hybrid can be used as a sensitive interface for electrochemical simultaneous and sensitive detection of Cd^{2+} and Pb^{2+}, giving limits of detection (LOD) of 29.9 μg L^{-1} for Cd^{2+}, and 10.6 μg L^{-1} for Pb^{2+}. Therefore, this work presented a simple and promising platform to electrochemical sensor for detecting heavy metal ions with high performance.
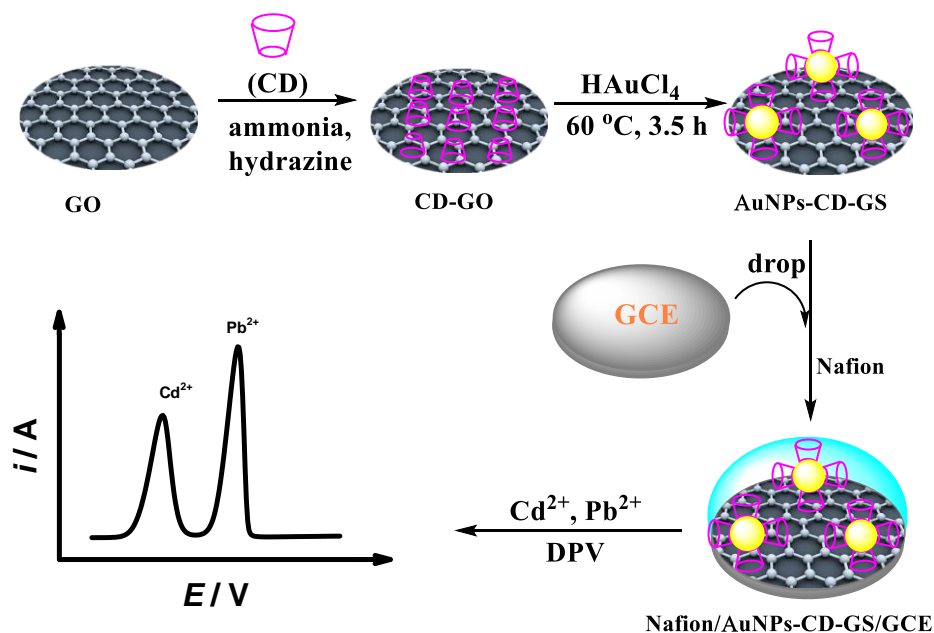
Scheme 1. Steps for preparing the AuNPs-CD-GS, electrochemical sensor and outputting the electrochemical signal.

2. MATERIALS AND METHODS

2.1. Instrumentation and chemicals

All electrochemical experiments were performed on a CHI660E electrochemical workstation (Shanghai ChenHua Instruments Co., China) and a conventional three-electrode electrolytic cell was used. A GCE with 3.0 mm diameter, a KCl-saturated calomel electrode and a platinum wire with 0.2 mm diameter served as the working electrode, reference electrode and the counter electrode, respectively. TEM (JEM-3010, Jeol, Japan) and SEM (JEM-6700F field emission scanning electron microscope) were applied to characterize the structure of composites. The elemental analysis results were tested by energy Dispersive X-ray Detector (EDX). FT-IR spectra was recorded from a KBr window by a Nicolet Nexus 670 FT-IR spectrophotometer. XPS was recorded from an Axis Ultra spectrometer (Kratos Analytical Ltd., Japan).

GO was obtained from Nanjing XFNANO Materials Tech. Co., Ltd. (Nanjing, China). Nafion (5 wt%) solution and gold(III) chloride trihydrate (≥99.9%) were provided by Sigma-Aldrich. β-CD was purchased from Shangdong Zhiyuan Biotechnology Company (China). All other reagents and solvents used in this work were of analytical grade or better quality. Double-distilled deionized water was used throughout the experiments. A 0.2 M acetic acid–sodium acetate (HAc/NaAc) buffer solution served as a supporting electrolyte during the analysis of metal ions. The real water samples were collected from Liuyang River which is in Changsha city, Hunan province, China. The water samples were purified by centrifuging and filtering, then diluted with HAc/NaAc buffer solution before for electrochemical analysis.

2.2. Preparation of CD-GS or AuNPs-CD-GS composites

After soaking in aqua regia (V_{HNO3}: V_{HCl} =1:3) and then rinsing with ultrapure water, the round bottomed flask was oven-dried prior to use. The CD-GS composite was prepared as reported before [25] and the preparation of AuNPs-CD-GS composite was similar with it. Briefly, 20 mL of 0.5 mg mL^{-1} GO and 20 mL of 80 mg mL^{-1} β-CD were mixed in a 100 mL round bottomed flask and ultrasonicated for 3 min. Then, added 140 μL of 28% NH$_3$·H$_2$O solution and 20 μL of 35% hydrazine solution, following by vigorously stirring for several minutes. Finally, different volumes (from 0 to 15.0 μL) of 0.01% HAuCl$_4$ solution was slowly added to the above solution and continued stirring to allow reaction at 60 °C for 3.5 h. After cooling down and filtrating with a membrane, the stable and different color from black to black-red dispersions were obtained.

2.3. Preparation of modified electrodes

Prior to modification, GCE was carefully polished with aqueous alumina slurries (Al$_2$O$_3$) and ultrasonically treated in ethanol and water to remove impurities as previous described [28-30]. Next, 2.5 μL of 0.5 mg mL^{-1} GS, CD-GS or AuNPs-CD-GS composite suspension was placed onto the cleaned GCE surface and dried at room temperature. Subsequently, 4 μL of 0.1% Nafion was casted on the electrode. After drying and washing with water, the modified electrode was utilized to following electrochemical studies.

2.4. Electrochemical measurement procedures

Differential pulse voltammetry (DPV) was used to the electrochemical measurement of Cd^{2+} and Pb^{2+} on the modified electrode. For cathodic preconcentration, the modified electrode was immersed into a 10 mL of 0.2 M HAc/NaAc buffer solution containing a certain amount of Cd^{2+} and Pb^{2+} under a constant potential at -1.2 V for 300 s to accumulate of heavy metal ions on the sensor under stirring condition. After stopped the stir, DPV from -1.0 to 0.2 V with 4 mV potential steps, 50 mV amplitude and 50 ms pulse width was conducted to record the stripping currents. The modified electrodes were renewed at 0.5 V for 80 s to remove the residual metals during solution-stirring.

3. RESULTS AND DISCUSSION

3.1. Characterizations of AuNPs-CD-GS composites

The synthesis procedure of AuNPs-CD-GS composites is shown in Scheme 1. It is a simple chemical method for synthesizing the AuNPs-CD-GS composites using the hydrazine to reduce the GO and HAuCl$_4$, meanwhile, the β-CD not only as a stabilizer, disperser, and reductant for forming dispersive AuNPs, but also as a linker to connect AuNPs and GS [26, 27]. Actually, the dispersion of AuNPs-CD-GS composites is very stable and can keep no precipitates at least three months. As shown

in Figure 1A and B, the AuNPs are homogeneous distributed on the prepared composites surface and the size of AuNPs is 15-18 nm. In addition, the EDX analysis and elemental mapping distributions of the AuNPs-CD-GS indicate that this composites contain the C, O and Au elements, and Au element was uniformly dispersed in this composites, as shown in Figure 1C-E.
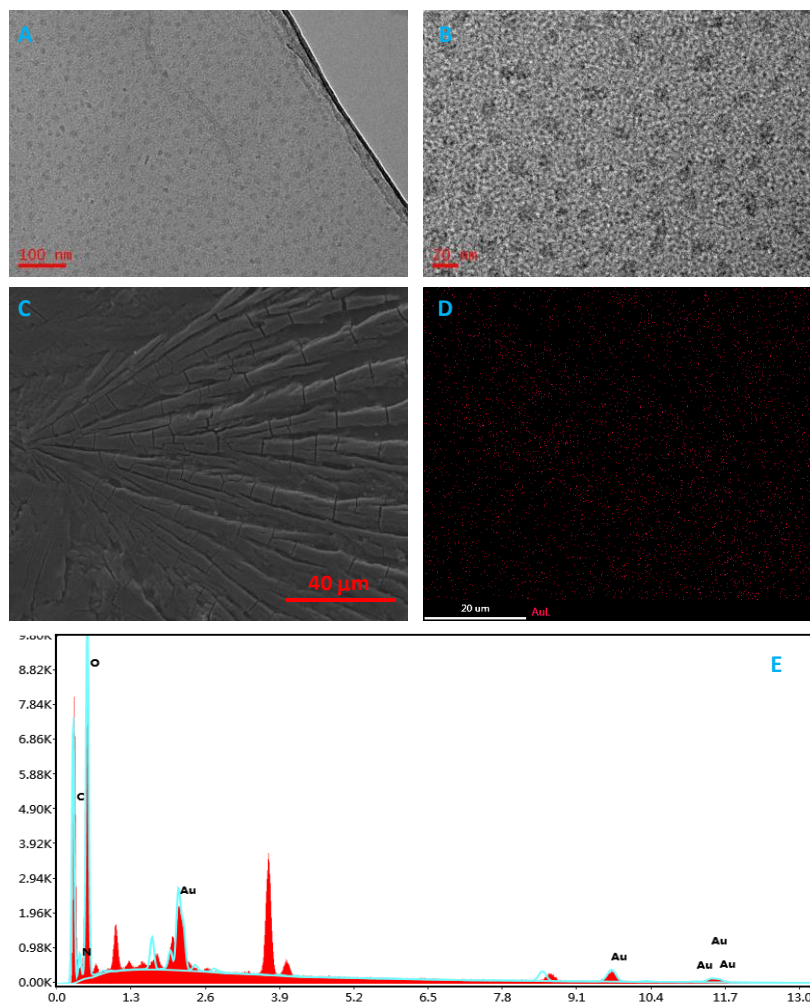

Figure 1. TEM images of AuNPs-CD-GS at different magnifications (A, B). SEM image (C) of AuNPs-CD-GS/GCE and its corresponding elemental map for Au-L (D) and EDX analysis (E).

Figure 2 displays the FT-IR spectrum of GO (a), CD-GS (b), AuNPs-CD-GS (c) and β-CD (d). Note that the carbonyl C=O peak at 1750 cm^{-1} for GO was disappeared after it reacted with the strong reducing agent–hydrazine [31]. It clearly confirms that the β-CD molecules of CD-GS and AuNPs-CD-GS are attached to the surface of them, due to the typical β-CD absorption features of the O-H stretching vibration peak at 3386 cm^{-1}, CH$_2$ stretching vibration peak at 2925 cm^{-1}, C-H/O-H bending vibration at 1416 cm^{-1}, the coupled C-O-C stretching/O-H bending vibration at 1155 cm^{-1}, and the coupled C-O/C-C stretching/O-H bending vibrations at 1027 cm^{-1} as well as the skeletal vibration of benzene at 1630 cm^{-1} for GO/GS [15, 25, 27]. While the XPS was used to further characterize the prepared the AuNPs-

CD-GS, as shown in Figure 3. The XPS results of AuNPs-CD-GS show the C 1s, O 1s and Au 4f peaks belonging to the AuNPs and CD-GS, respectively. All these results clarify that β-CD molecules are successfully attached onto the surface of AuNPs-CD-GS.
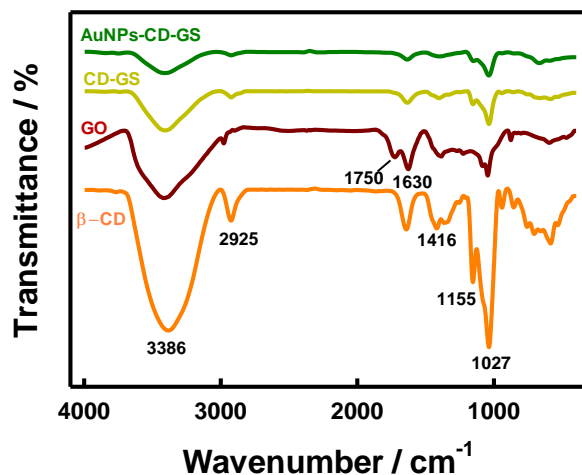

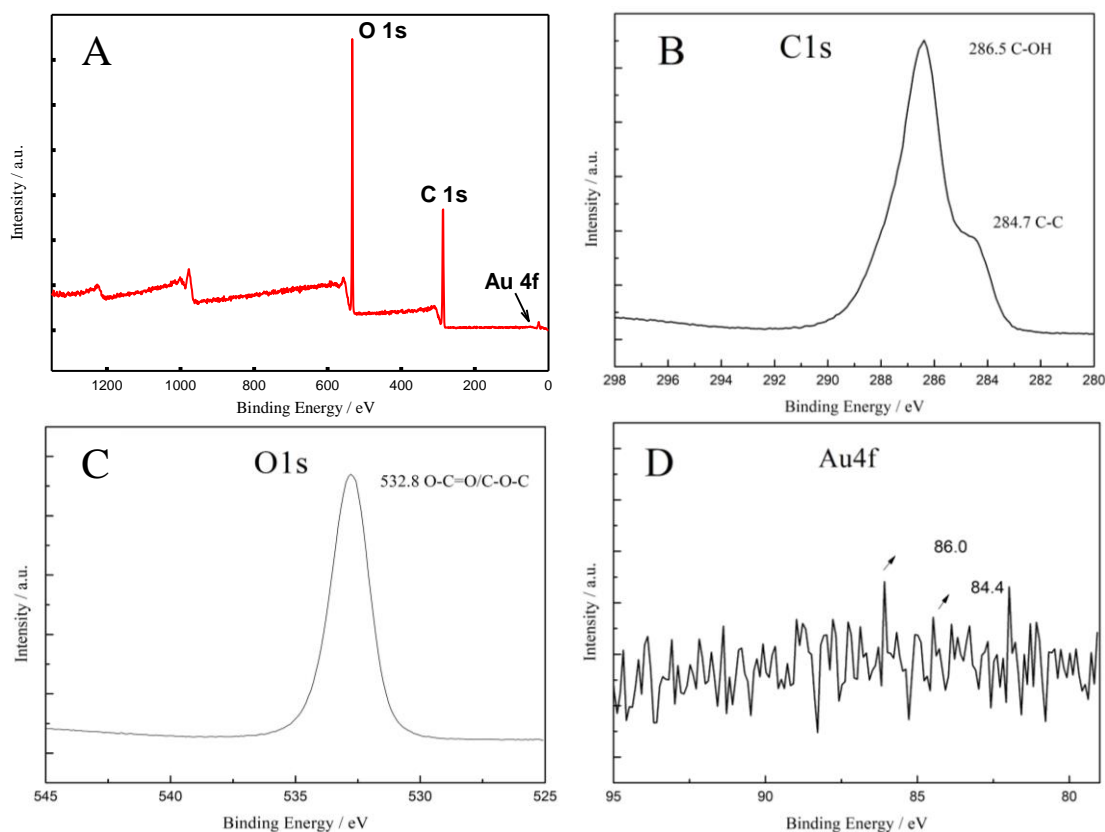**Figure 2.** FT-IR spectra of GO (a), CD-GS (b)，AuNPs-CD-GS (c) and β-CD (d).

Figure 3. XPS spectrum of CD-GS-AuNPs (A): C 1s (B), O 1s (C) and Au 4f (D).

3.2. Elelctrochemical performance of the different modified electrodes

Figure 4 shows that the DPV response at the bare GCE, Nafion/GS/GCE, Nafion/CD-GS/GCE and Nafion/AuNPs-CD-GS/GCE recorded from -1.0 V to -0.2 V in 0.2 M HAc-NaAc (pH= 5.0) containing 400 μg L^{-1} Cd^{2+} and Pb^{2+}. There are no obviously distinction of the bare GCE and Nafion/GS/GCE while a slight enhanced signal was obtained on the Nafion/CD-GS/GCE. Since the β-CD has multiple hydroxyl groups could complex with Cd^{2+} and Pb^{2+} and then enrich on the surface of Nafion/CD-GS/GCE [19], but β-CD itself has poor conductivity resulting in the signal just enhanced slightly [25]. In contrast, the Nafion/AuNPs-CD-GS/GCE has a further enhanced signal than the other three electrodes, highlighting the importance of the AuNPs in this complex, since the AuNPs can effectively enhance the conductivity of Nafion/AuNPs-CD-GS/GCE. And the current peaks of Cd^{2+} and Pb^{2+} appeared at -0.84 V and -0.60 V, respectively. In our protocol, β-CD not only acts as a stabilizer, disperser, and reductant for forming dispersive AuNPs, but also as a linker to connect AuNPs and GS through hydrogen bonds between GS and hydroxyl groups of β-CD. Furthermore, it is very important for amplifying the electrochemical signal as well as improving the sensitivity of this sensor, because both AuNPs and GS can be modified with β-CD, which can provide more sites for metal ions attachment through forming stable inclusive complex between β-CD and metal ions. Therefore, AuNPs-CD-GS modified electrode will have a good chance to develop a high sensitivity and enrichment ability toward metal ions.
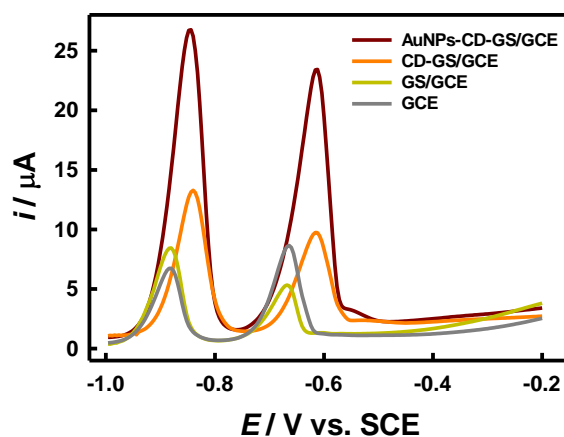

Figure 4. DPV of GO, CD-GS and AuNPs-CD-GS hybrid modified electrodes in 0.2 M HAc-NaAc (pH= 5.0) containing 400 μg L^{-1} Cd^{2+} and Pb^{2+}. Deposition potential: -1.1 V. Deposition time: 240 s.

3.3. Optimization of the determination conditions

To acquire the maximum sensitivity of the AuNPs-CD-GS hybrid modified electrode for Cd^{2+} and Pb^{2+}, several important parameters were explored as follow. Firstly, the volume of 0.01% $HAuCl_4$ solution used to synthesize AuNPs-CD-GS was optimized. Figure 5A shows that peak currents of Cd^{2+} and Pb^{2+} increased with the increase of $HAuCl_4$ volume, since larger volumes of 0.01% $HAuCl_4$ solution can produce more AuNPs for enhanced conductivity of AuNPs-CD-GS and obtained larger stripping

peaks. Whereas the peak currents of Cd^{2+} and Pb^{2+} decreased after the $HAuCl_4$ volume larger than 5.0 μL, because excess AuNPs led to the evolution of hydrogen on the Nafion/AuNPs-CD-GS/GCE at the cathodic deposition potential (-1.2 V) [32, 33], which can decrease the enrichment of metal ions. Thus, 5.0 μL of 0.01% $HAuCl_4$ solution is the best to maximize the signal.

Secondly, the effect of pH value of HAc/NaAc buffer solution was investigated in the range from 3.0 to 6.0, as shown in Figure 5B. The stripping peak currents of Cd^{2+} and Pb^{2+} increase with increasing the pH from 3.0 to 5.0 and then reach a maximum response at pH 5.0, while decrease is displayed from 5.0 to 6.0. The reason may be the deprotonation of β-CD enhanced with increasing pH from 3.0 to 5.0 leading to the strong adsorption towards the metal ions, whereas the higher pH caused the hydrolysis reaction for Cd^{2+} and Pb^{2+} and decreasing the absorption amount as well as the stripping currents [1]. Therefore, pH 5.0 of HAc/NaAc buffer solution was used for the following measurements.

Thirdly, the effect of the deposition potential and times on the stripping peak currents were explored in pH 5.0 HAc/NaAc buffer solution, as shown in Figure 5C and Figure 5D. It can be found that the stripping peak currents for Cd^{2+} and Pb^{2+} increase with the deposition potential decreasing from -1.0 to -1.2 V, but the peak currents decreased after the potential negative than -1.2 V due to the competitive generation of hydrogen [17]. The electrochemical response of Cd^{2+} and Pb^{2+} enhanced with the increase of the deposition time from 120 s to 300 s. However, there was no obvious increase of stripping peak current with further increase of deposition time. Hence, the optimal deposition potential and time was -1.2 V and 300 s, respectively.
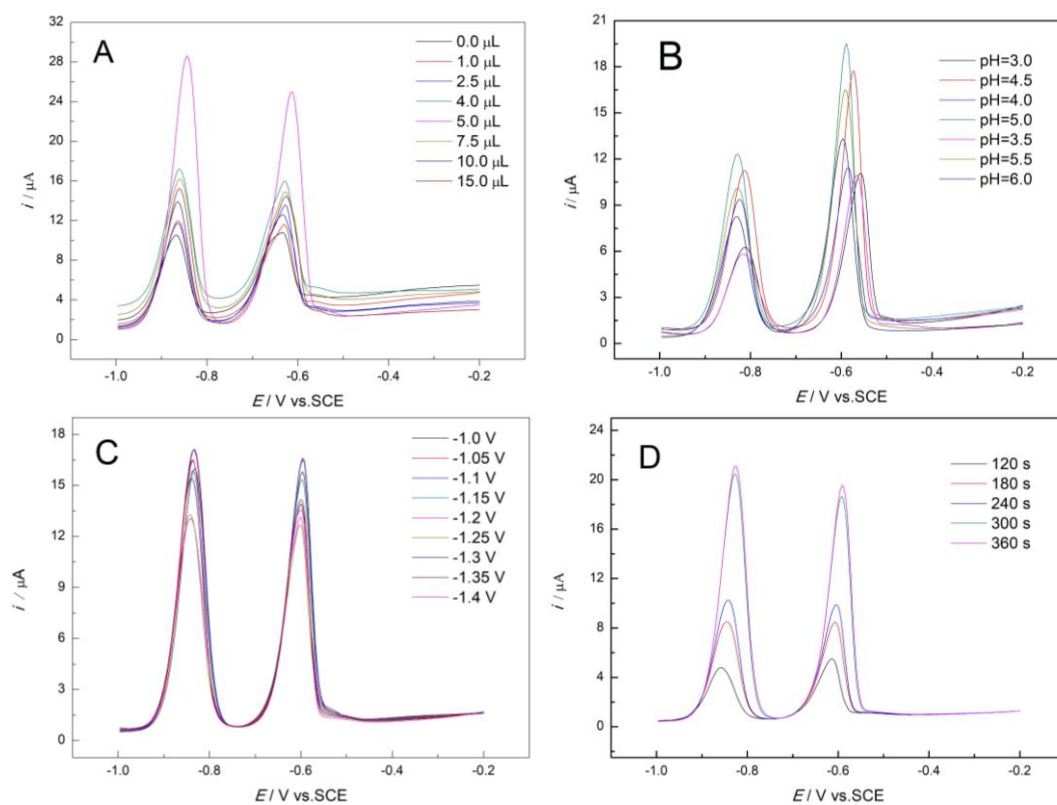

Figure 5. The effect concentration of $HAuCl_4$ (A), effect of pH (B), effect of deposition potential (C) and deposition time (D) on the stripping peak of 400 μg L^{-1} Cd^{2+} and Pb^{2+} at the Nafion/AuNPs-CD-GS/GCE.

3.3. The electrochemical detection of Cd^{2+} and Pb^{2+}

Under the optimum conditions, we used the as-prepared Nafion/AuNPs-CD-GS/GCE to detect the Cd^{2+} and Pb^{2+} individually and simultaneously in 0.2 M pH 5.0 HAc/NaAc buffer solution. The linear responses of stripping peak currents to the Cd^{2+} and Pb^{2+} concentration both from 40 µg L^{-1} to 1200 µg L^{-1} and the LOD was 24.8 µg L^{-1} and 15.8 µg L^{-1} (*S/N*=3) (Figure 6A, B), respectively. The analytical property of the Nafion/AuNPs-CD-GS/GCE for the simultaneous detection of Cd^{2+} and Pb^{2+} with increasing concentrations of these both metal ions is also shown in Figure 6C. The LOD of Cd^{2+} and Pb^{2+} was 29.9 µg L^{-1} and 10.6 µg L^{-1} (*S/N*=3), respectively. The analytical performance of this sensor is comparable and offers a wider range than the previous reports, as shown in Table 1. The almost unchanging LODs and sensitivity for simultaneous detection of these two ions indicate that this protocol can be applied for the individual and simultaneous detection of Cd^{2+} and Pb^{2+}. The selectivity and reproducibility of this sensor were also investigated. Nine different metal ions each at a 10-fold concentration of Cd^{2+} and Pb^{2+} were added and the responses was less than 10% with added interfering metal ions as shown in Figure 6D. The reproducibility of this sensor was investigated by five different Nafion/AuNPs-CD-GS/GCE to detect the Cd^{2+} and Pb^{2+}, giving RSDs of 3.6% and 2.9%, respectively. Meanwhile, the RSDs of simultaneous detection of Cd^{2+} and Pb^{2+} were 4.1% and 3.2%, validating great reproducibility of this proposal sensor.
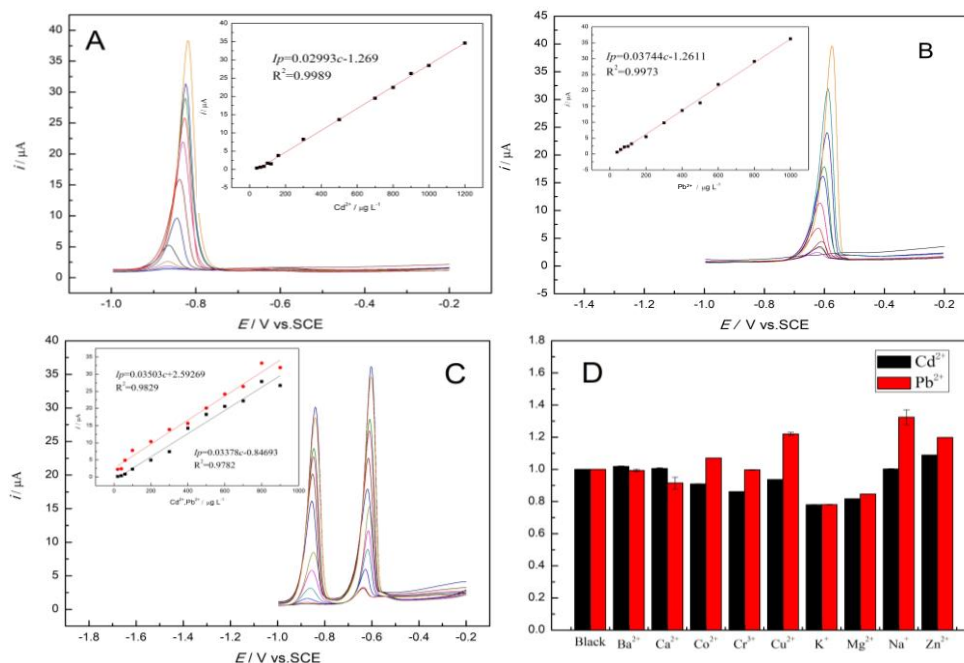

Figure 6. DPV for individual detection of Cd^{2+} (A) and Pb^{2+} (B) at different concentrations under the optimized conditions. The insets are the corresponding calibration curves of the peak currents to the concentration of Cd^{2+} and Pb^{2+}, respectively. (C) Simultaneous detection of Cd^{2+} and Pb^{2+} at different concentrations under the optimized conditions. The insets are the corresponding calibration plots. (D) Interference experiments on the stripping peak currents for simultaneous detection of Cd^{2+} and Pb^{2+} with different metal ions (10-fold concentration) under optimal conditions. The red and black columns represent the i_{Pb+M}/i_{Pb} and i_{Cd+M}/i_{Cd}, respectively. M means the interferential metal ions.

Table 1. Comparison of this method with some previous electrochemical methods.

Modified Electrode	Method	Linear range (µg L^{-1})		LOD (µg L^{-1})		Reference
		Cd^{2+}	Pb^{2+}	Cd^{2+}	Pb^{2+}	
GO-Fe$_3$O$_4$-PAMAM/GCE	SWV	0.4-140	0.2-120	0.07	0.13	[11]
PA/PPy/GO	DPV	5-150	5-150	2.13	0.41	[34]
Bi/Nafion/OPPy-MES/GCE	SWV	0.1-25	0.05-35	0.04	0.03	[35]
Bi/CMWCNTs-CD-Nafion/GCE	SWV	1-100	1-100	0.13	0.13	[36]
Fe$_3$O$_4$/MWCNTs/LSG/CS/GCE	SWV	1-200	1-200	0.07	0.1	[37]
AuNPs-CD-GS/GCE	SWV	40-1200	40-1200	24.8	10.6	This Work

DPV: differential pulse voltammetry; LSG: laser scribed graphene; MES: 2-mercaptoethanesulfonate; OPPy: overoxidation of polypyrrole; PA: phytic acid; PAMAM: poly(amidoamine); PPy: polypyrrole.

3.4. Simultaneous determination of Cd^{2+} and Pb^{2+} in practical samples

The Nafion/AuNPs-CD-GS/GCE was also examined the real applicability for simultaneous determination of Cd^{2+} and Pb^{2+} in water from local river. As listed in Table 2, the acceptable average recoveries for Cd^{2+} and Pb^{2+} are obtained (within ±7% RSD), confirming that this proposal sensor can be used for simultaneous determination of Cd^{2+} and Pb^{2+} in real water samples.

Table 2. Simultaneous determination of Cd^{2+} and Pb^{2+} in real water samples by our method.

Sample	Added (µg L^{-1})		Cd^{2+}			Pb^{2+}		
	Cd^{2+}	Pb^{2+}	Found (µg L^{-1})	Recovery (%)	RSD (%)	Found (µg L^{-1})	Recovery (%)	RSD (%)
River water	0	0	0	-	-	0	-	-
	50	50	47	94	-6.8	49	98	-2.4
	100	100	107	107	6.9	102	102	2.1

4. CONCLUSIONS

In summary, a sensitive electrochemical sensing platform based on AuNPs-CD-GS nanocomposite was applied for the individual/simultaneous determination of Cd^{2+} and Pb^{2+} with wide linear detection range (40 - 1200 µg L^{-1}) and low LOD, which performed better than many reported previously. Moreover, simultaneous determination of Cd^{2+} and Pb^{2+} in real water samples by our method presents good recoveries. The disperse AuNPs-CD-GS are fabricated by a simple one-pot synthesis using

hydrazine and β-CD as reducing agents to reduce the GO and gold ions and the concentration of HAuCl$_4$ was optimized. This nanocomposite not only presents the excellent electrical properties of AuNPs and GS but also shows high capture capability due to the strong adsorption uptake of Cd^{2+} and Pb^{2+} on β-CD. This multi-functional nanocomposite was firstly used in electrochemical sensor for detection of Cd^{2+} and Pb^{2+}, which offers a great potential sensing platform for environmental heavy metals and other analytical applications.

CONFLICTS OF INTEREST

The authors declare no conflict of interest.

References

1. M. Lu, Y. Deng, Y. Luo, J. Lv, T. Li, J. Xu, S. W. Chen and J. Wang, *Anal. Chem.*, 91 (2019) 888.
2. J. H. Park, G. Yeom, D. Hong, E. J. Jo, C. J. Park and M. G. Kim, *Sensors*, 19 (2019).
3. B. M. Jun, S. Kim, Y. Kim, N. Her, J. Heo, J. Han, M. Jang, C. M. Park and Y. Yoon, *Chemosphere*, 231 (2019) 82.
4. F. Mo, Z. Ma, T. Wu, M. Liu, Y. Zhang, H. Li and S. Yao, *Sens. Actuators B: Chem.*, 281 (2019) 486.
5. L. Zhang, D. Peng, R.-P. Liang and J.-D. Qiu, *Trends Anal. Chem.*, 102 (2018) 280.
6. S. A. Rezvani and A. Soleymanpour, *J. Chromatogr. A.*, 1436 (2016) 34.
7. M. Shen, L. Chen, W. Han and A. Ma, *Microchem. J.*, 139 (2018) 295.
8. B. Bansod, T. Kumar, R. Thakur, S. Rana and I. Singh, *Biosens. Bioelectron.*, 94 (2017) 443.
9. F. Vajedi and H. Dehghani, *Mater. Sci. Eng. B*, 243 (2019) 189.
10. S. Duan and Y. Huang, *J. Electroanal. Chem.*, 807 (2017) 253.
11. M. Baghayeri, H. Alinezhad, M. Fayazi, M. Tarahomi, R. Ghanei-Motlagh and B. Maleki, *Electrochim. Acta*, 312 (2019) 80.
12. Y. Li, Y. Chen, H. Yu, L. Tian and Z. Wang, *Trends Anal. Chem.*, 98 (2018) 190.
13. G. Aragay, J. Pons and A. Merkoçi, *Chem. Rev.* , 111 (2011) 3433.
14. Y. Zhao, Y. Huang, H. Zhu, Q. Zhu and Y. Xia, *J. Am. Chem. Soc.*, 138 (2016) 16645.
15. M. Ma, T. Zhe, W. Song, P. Guo, J. Wang and J. Wang, *Sens. Actuators B: Chem.*, 253 (2017) 818.
16. X. Qin, A. Xu, L. Liu, Y. Sui, Y. Li, Y. Tan, C. Chen and Q. Xie, *Biosens. Bioelectron.*, 91 (2017) 321.
17. F. Zhan, F. Gao, X. Wang, L. Xie, F. Gao and Q. Wang, *Microchim. Acta*, 183 (2016) 1169.
18. R. K. S. Rathour, J. Bhattacharya and A. Mukherjee, *J. Mol. Liq.*, 282 (2019) 606.
19. X. Qin, L. Bai, Y. Tan, L. Li, F. Song and Y. Wang, *Chem. Eng. J.* , 372 (2019) 1007.
20. T. T. Tung, M. J. Nine, M. Krebsz, T. Pasinszki, C. J. Coghlan, D. N. H. Tran and D. Losic, *Adv. Funct. Mater.*, 27 (2017) 1702891.
21. M. Pumera, *Chem. Soc. Rev.*, 39 (2010) 4146.
22. V. Georgakilas, J. N. Tiwari, K. C. Kemp, J. A. Perman, A. B. Bourlinos, K. S. Kim and R. Zboril, *Chem. Rev.*, 116 (2016) 5464.
23. A. Ambrosi, C. K. Chua, A. Bonanni and M. Pumera, *Chem. Rev.*, 114 (2014) 7150.

24. P. T. Yin, S. Shah, M. Chhowalla and K.-B. Lee, *Chem. Rev.*, 115 (2015) 2483.
25. Y. Guo, S. Guo, J. Ren, Y. Zhai, S. Dong and E. Wang, *ACS Nano*, 4 (2010) 4001.
26. T. Wu, Z. Liu, Y. Guo and C. Dong, *J. Electroanal. Chem.*, 759 (2015) 137.
27. Q. Xue, Z. Liu, Y. Guo and S. Guo, *Biosens. Bioelectron.*, 68 (2015) 429.
28. X. Qin, X. Zhang, M. Wang, Y. Dong, J. Liu, Z. Zhu, M. Li, D. Yang and Y. Shao, *Anal. Chem.*, 90 (2018) 11622.
29. X. Qin, Y. Dong, M. Wang, Z. Zhu, M. Li, X. Chen, D. Yang and Y. Shao, *Sci. China Chem.*, 61 (2018) 476.
30. X. Qin, L. Wang and Q. Xie, *Sensors* 16 (2016) 1342.
31. T. Feng, X. Qiao, H. Wang, Z. Sun, Y. Qi and C. Hong, *J. Mater. Chem. B*, 4 (2016) 990.
32. T. Mitsudome and K. Kaneda, *Green Chem.*, 15 (2013) 2636.
33. B. G. Ershov, E. V. Abkhalimov, R. D. Solovov and V. I. Roldughin, *Phys. Chem. Chem. Phys.*, 18 (2016) 13459.
34. H. Dai, N. Wang, D. Wang, H. Ma and M. Lin, *Chem. Eng. J.*, 299 (2016) 150.
35. L. Chen, Z. Li, Y. Meng, P. Zhang, Z. Su, Y. Liu, Y. Huang, Y. Zhou, Q. Xie and S. Yao, *Sens. Actuators, B*, 191 (2014) 94.
36. G. Zhao, H. Wang, G. Liu and Z. Wang, *Int. J. Electrochem. Sci.*, 11 (2016) 8109.
37. Z. Xu, X. Fan, Q. Ma, B. Tang, Z. Lu, J. Zhang, G. Mo, J. Ye and J. Ye, *Mater. Chem. Phys.*, 238 (2019) 121877.